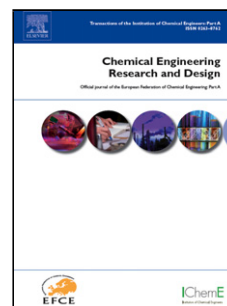


Journal Pre-proof

Laser Doppler electrophoresis and electro-osmotic flow mapping for the zeta potential measurement of positively charged membrane surfaces

Matthew Walters Saif Al Aani Peter P. Esteban Paul M. Williams
Darren L. Oatley-Radcliffe



PII: S0263-8762(20)30179-9

DOI: <https://doi.org/doi:10.1016/j.cherd.2020.04.022>

Reference: CHERD 4073

To appear in: *Chemical Engineering Research and Design*

Received Date: 7 January 2020

Revised Date: 18 March 2020

Accepted Date: 7 April 2020

Please cite this article as: Walters, M., Aani, S.A., Esteban, P.P., Williams, P.M., Oatley-Radcliffe, D.L., Laser Doppler electrophoresis and electro-osmotic flow mapping for the zeta potential measurement of positively charged membrane surfaces, *Chemical Engineering Research and Design* (2020), doi: <https://doi.org/10.1016/j.cherd.2020.04.022>

This is a PDF file of an article that has undergone enhancements after acceptance, such as the addition of a cover page and metadata, and formatting for readability, but it is not yet the definitive version of record. This version will undergo additional copyediting, typesetting and review before it is published in its final form, but we are providing this version to give early visibility of the article. Please note that, during the production process, errors may be discovered which could affect the content, and all legal disclaimers that apply to the journal pertain.

© 2020 Published by Elsevier.

1 Laser Doppler electrophoresis and electro-osmotic flow mapping for the zeta 2 potential measurement of positively charged membrane surfaces

3
4 Matthew Walters, Saif Al Aani, Peter P. Esteban, Paul M. Williams, Darren L. Oatley-Radcliffe *

5
6 Energy Safety Research Institute (ESRI), College of Engineering, Swansea University, Fabian Way,
7 Swansea SA1 8EN, UK

8 * Corresponding author

9 E-mail address: D.L.Oatley@swansea.ac.uk (D.L. Oatley-Radcliffe)

10 11 12 **Abstract**

13 Successful characterization of membranes is of paramount importance for the development and
14 improvement of novel membranes and membrane processes. The characterisation of membrane
15 charge is key to understanding charge interactions between the process stream and the membrane
16 and is typically represented by the surface zeta potential. In a previous paper [1], a novel technique
17 employing an Uzigirs dip cell arrangement used in conjunction with Laser Doppler Electrophoresis
18 was used to characterize the surface of several negatively charged membranes. In this paper,
19 positively charged modified PTFE membranes are fabricated and the novel zeta potential
20 measurement technique is utilised to quantify the resultant membrane charge by use of a positively
21 charged amidine tracer particle. The amidine particles were characterised and shown to have a
22 positive zeta potential of 12.4 mV for the experimental conditions used. A comparative analysis was
23 made between the novel laser Doppler electrophoresis measurements and tangential streaming
24 potential measurements for the positive membrane and the agreement was good. The phase plot
25 and mobility-displacement were of good quality for the data set, with the surface equivalent
26 mobility being $0.632 \mu\text{mcm/Vs}$ with $R^2 = 0.977$. In addition, a series of experiments were conducted
27 to explore the operating envelope and highlight the pitfalls of the technique, i.e. oppositely charged
28 particles to the surface should not be used. Overall, this work expands the application of the novel
29 zeta potential measurement technique to span all membrane charge types. Thus providing a real
30 benefit to the practicing scientist or engineer by having a reliable, fast and simple zeta potential
31 technique that uses only a very small membrane sample.

32
33
34 **Key words:** Membrane, charge, zeta potential, positive, electrophoresis

35 36 37 38 **1.0 Introduction**

39 Membrane technology is now embedded across a wide range of industrial applications including
40 water purification, pharmaceutical, biotechnology, petrochemical and textiles to name a few [2-5].
41 The general role of membranes is to separate, fractionate, concentrate or remove materials such as
42 microorganisms, fine particles, proteins, nucleic acids, sugars, other organics and mineral solutes
43 from various solutions [6-8]. The main separation mechanisms for membrane filtration are steric and
44 Donnan based interactions [9-12]. Steric interactions at membrane surfaces are very well
45 understood and easily measurable [13]. Charge effects are far more complex and a detailed
46 examination of charge behaviour provides greater knowledge of the solute-solution-surface

47 mechanistic interactions, which leads to a better understanding of the subsequent membrane
48 process performance.

49
50 Semipermeable membranes generate an electrical surface charge when contacted by a solution.
51 Ions and molecules from the solution interact with the surface functional groups of the membrane
52 leading to a chemical dissociation from the membrane surface resulting in charge generation. At the
53 same time, ions in the contacting solution may adsorb on to the membrane surface, also generating
54 a surface charge. Typical adsorbed materials include polyelectrolytes, ions, macromolecules and
55 surfactants. The spacial distribution and concentration of these dissolved solutes and ions at the
56 membrane interface is ordered and forms the classical electrical double layer [14-15]. The shear
57 plane separates the stationary phase from the mobile phase of the electrical double layer and is
58 critical to all fundamental models describing the electrical double layer. Zeta (ζ) potential is defined
59 as the electrical potential at the shear plane. The zeta potential is a relatively simple electrokinetic
60 phenomenon often used to quantify membrane surface charge in place of the membrane surface
61 potential which, by comparison, is difficult to measure. Zeta potential measurements are important
62 when determining membrane separation mechanisms, membrane fouling, ageing, cleaning, and
63 functionalization [16-18]. Zeta potential is normally derived from either sedimentation potential,
64 streaming potential, electrophoresis or electro-osmosis, with streaming potential often being the
65 preferred option due to the methods inherent simplicity. A more detailed explanation of streaming
66 potential, used in this study, is provided in the theoretical descriptions and each of the other
67 phenomena is described in detail elsewhere [19-20].

68
69 Advances in Laser Doppler Electrophoresis (LDE) technology and Dynamic Light Scattering (DLS) have
70 now opened up a new methodology to measure surface zeta potential through electro-osmotic flow
71 mapping and using an Uzgiris dip cell [21-22]. In a previous paper [1], this novel method for the
72 determination of membrane surface zeta potentials was applied to measure the surface charge of
73 ultrafiltration, nanofiltration and reverse osmosis membranes. The technique specifically examines
74 the electrophoretic mobility of carboxylated polystyrene tracer microparticles suspended in the
75 contacting electrolyte solution. High quality regression correlations ($R^2 > 0.95$) were obtained under
76 most operating conditions and excellent agreement was obtained when comparing zeta potential
77 results to the traditional tangential streaming potential measurement. The methodology has several
78 advantages over traditional surface potential methods. These include:

- 79
- 80 ▪ Only a very small membrane sample is required when compared to other techniques, for
81 example: The SurPASS instrument for zeta potential measurement uses either a clamping
82 cell or adjustable gap cell with sample areas of 55 x 25 mm and 25 x 5 mm respectively [30].
83 This measurement uses a sample of 3.5 x 5 mm only. This is particularly useful in the
84 laboratory and early phase development of new membranes.
 - 85 ▪ The technique can be applied to any class of liquid phase membrane, i.e. microfiltration,
86 ultrafiltration, nanofiltration or reverse osmosis membrane.
 - 87 ▪ The measurement equipment is more economic when compared to other commercially
88 available devices.
 - 89 ▪ The measurement equipment is multifunctional, i.e. performs zeta potential measurements
90 for particles and surfaces as well as particle size characterisation.

91
92 While the technique offers a simple and economic method for the characterisation of membrane
93 zeta potential, there was one major drawback. Careful consideration is required for the selection of
94 appropriate tracer particles. The sole aim of these particles is to scatter light: chemical functionality

95 or surface chemistry does not affect the measurement. However, an essential criterion is that the
96 tracer particles do not interact with the sample surface [23]. Due to the requirement for a mobile
97 particle, in this case a negatively charged carboxylated polystyrene latex particle, the technique was
98 limited to the characterisation of negatively charged surfaces only. In this paper, the novel technique
99 for measuring membrane surface zeta potential has been expanded by inclusion of an alternate
100 mobile particle which allows for the measurement of positively charged surfaces, thus allowing the
101 measurement technique to be employed across the full spectrum of membrane charge.

102 **2.0 Theoretical Descriptions**

103 The theoretical descriptions used in this paper have been detailed elsewhere [1] and will only briefly
104 be discussed here to provide appropriate background to complement the methods used.

105 **2.1 Description of Zeta potential**

106 The classical Gouy-Chapman-Stern-Grahame model describes the distribution of charge within the
107 electrical double layer, see Figure 1. There are two clearly defined zones within the electrical double
108 layer;

- 109 ▪ the stern layer; which lies between the membrane and the outer Helmholtz plane is
110 immobile, ions from the surrounding liquid bind at the solid interface, and
- 111 ▪ the diffuse layer; beyond the outer Helmholtz plane which is mobile, ions move freely by
112 thermal motion.

113 The plane of shear separates these two layers, with the first layer known as the inner Helmholtz
114 plane (IHP) and the second known as the outer Helmholtz plane (OHP). Extending beyond the OHP
115 into the bulk solution is the diffuse layer, where Brownian motion applies. Three different charge
116 potentials are denoted in Figure 1, namely: the membrane surface potential (Ψ_0), the potential at
117 the IHP (Ψ_{IHP}) and OHP (Ψ_{OHP}). The magnitude of the potential decreases linearly from the IHP to the
118 OHP. The zeta potential (ζ) is measured at the shear plane.

119 **2.2 Zeta potential measurement**

120 Only descriptions related to the techniques in this paper will be discussed here, for further
121 information on other techniques available see [13].

122 **2.2.1 Tangential streaming potential measurements**

123 Zeta potential measurements derived from streaming potential are either transversal or tangential
124 [24]. For transversal measurements flow travels through the membrane pores, while for tangential
125 measurements flow travels parallel to the membrane surface. Tangential streaming potential is the
126 most commonly used method to measure zeta potential [25] and a wealth of information related to
127 this technique is available throughout the literature.

128 Two identical membrane active layers are arranged to face each other separated by spacers to form
129 a discrete flow channel. An electrolyte solution is pumped through the channel at a given flow rate
130 delivering a fixed hydrostatic pressure gradient. The charge density of the membrane surface causes
131 the counter ions to rearrange and excess ions are drawn towards the downstream (low-pressure)
132 side of the channel by shear flow action. The difference in concentration of counter ions from one
133 end of the channel to the other generates an induced electrical current known as the streaming
134 current. The potential difference resulting from the streaming current is measured and divided by
135 the pressure drop along the channel to form the potential coefficient.

$$142 \quad \phi_{st} = \Delta V / \Delta P \quad (1)$$

143

144 where ΔV is the potential difference and ΔP is the pressure gradient. Zeta potential is then
145 calculated from the streaming potential using the Smoluchowski equation.

146

$$147 \quad \zeta = \phi_{st} \frac{\eta}{\epsilon \epsilon_0} K_B \quad (2)$$

148

149 where ϵ is the dielectric constant of the dispersant, ϵ_0 is the permittivity of free space, η is the
150 apparent viscosity, and K_B is the conductivity of the solution. Note that electrolyte concentrations at
151 or less than 10^{-3} M are commonly used to avoid surface conductivity issues.

152

153 2.2.2 Laser Doppler Electrophoresis

154 Laser Doppler electrophoresis is dependent on the frequency of scattered laser light as a function of
155 particle velocity – known as the Doppler shift. This method has been used to study the diffusion of
156 particles in solution [26]. Many colloidal particles obtain a surface charge in solution and subjecting
157 colloidal particles to non-diffusional motion, from electric fields, leads to a phenomena known as
158 Doppler shift. This includes motion attributed to both diffusion and the induced electrophoretic
159 mobility. The velocity and direction of the resultant movement is a function of the suspending
160 medium, the electric field strength and the particle charge. The zeta potential is defined in terms of
161 electrophoretic mobility U_E by the Henry equation:

162

$$163 \quad U_E = \frac{2\epsilon\epsilon_0 F(\kappa a)}{3\eta} \zeta \quad (3)$$

164

165 where $F(\kappa a)$ is the Henry function, κ the inverse of the Debye length and a the particle radius
166 [22,27]. Two main assumptions are usually made for $F(\kappa a)$; either $F(\kappa a) = 1.0$ (the Debye
167 approximation) or $F(\kappa a) = 1.5$ (the Smoluchowski approximation) [28]. $F(\kappa a)$ is dependent on the
168 electrolyte used and the size of the colloid. For this work the Smoluchowski approximation was
169 employed, which is applicable to particles greater than 100 nm, aqueous solution, and ionic strength
170 greater than 10^{-3} M.

171

172 Phase Analysis Light Scattering (PALS) was measured and the frequency shift resulting from changes
173 in electrophoretic velocity v is given by:

174

$$175 \quad \Delta v = 2U_E \frac{\sin(\theta/2)}{\lambda} \quad (4)$$

176

177 where λ is the laser wavelength and θ is the angle of scatter [22,27].

178

179 2.2.3 Electro-osmotic flow mapping

180 Electro-osmosis is defined as the flow of a liquid through stationary particles in response to an
181 applied electric field. Electro-osmotic flow can be used with mobile tracer particles to evaluate
182 surface zeta potential. The surface in question, in this case a membrane, is fixed to a sample holder
183 and placed in an Uzgiris electrode in a cuvette, see Figure 2. When the electric field is switched on,
184 the motion of the particles is recorded using PALS. Electro-osmotic flow mapping characterises the
185 flow in the half space outside the slipping plane. To do this, measurements are taken at various
186 displacements y_i , normal to the membrane surface [21]. The slipping plane of the surface is
187 assumed to coincide with the test surface at the plane of $y = 0$.

188 Assuming zero backpressure and Stokes flow the linearized Navier-Stokes equation is given as:

189

$$190 \quad \rho v = \eta \left[\frac{d^2 v}{dx^2} + \frac{d^2 v}{dy^2} \right] \quad (5)$$

191

192 Where ρ is the fluid density, η the apparent viscosity and $v(t,x,y)$ the component of fluid velocity
193 parallel to the boundary. The y co-ordinate is perpendicular to the boundary and the x co-ordinate is
194 parallel. Continuity implies that v is not a function of x as no flow perpendicular to the boundary is
195 expected. The equation simplifies to:

196

$$197 \quad v = k \left[\frac{d^2 v}{dy^2} \right] \quad (6)$$

198

199 where $k = \eta/\rho$ (kinematic viscosity). Initial conditions are set as $v(0,y) = 0$ with the boundary
200 condition $v(t,0) = v_{eo}$, where v_{eo} is the fluid velocity at the boundary. However, the homogenous
201 initial conditions and Dirichlet boundary conditions are problematic on the half line $(0, \infty)$ but have
202 a Green function solution with the closed form:

203

$$204 \quad v(y,t) = \int_0^\infty \frac{1}{\sqrt{4\pi k(t-s)^3}} \exp\left(-\frac{y^2}{4k(t-s)}\right) v_{eo} ds \quad (7)$$

205

206 and solution:

207

$$208 \quad v(y,t) = v_{eo} \left[1 - \operatorname{erf}\left(\frac{y}{2\sqrt{kt}}\right) \right] \quad (8)$$

209

210 where erf is the error function. For $y \geq 750\mu\text{m}$ for $t \geq 75\text{ms}$ or $y \geq 1.5\text{mm}$ for $t \geq 300\text{ms}$, the
211 bracketed terms do not apply as $\operatorname{erf}\left(\frac{y}{2\sqrt{kt}}\right) \rightarrow 0$. For surface zeta potential measurements, the main
212 focus is in the y -axis intercept, however, since the measured value consists of both electroosmotic
213 and electrophoretic contributions, an estimate of the tracer velocity v_{ep} itself is also required.
214 Electrophoretic motion is recorded at set time intervals using PALS; therefore, the Navier-Stokes
215 equation can be fitted to measurements of $v_i(y_i)$ at various displacements and y_i can be
216 extrapolated to the y -axis intercept:

217

$$218 \quad v_{eo} = -\text{Intercept} + v_{ep} \quad (9)$$

219

220 The zeta potential ζ is then a function of the flow at the slipping plane v_{eo} by:

221

$$222 \quad \frac{v_{eo}}{E_x} = \frac{\epsilon \epsilon_0}{\eta} \zeta \quad (10)$$

223

224 where E_x is the electric field strength.

225

226

227 3.0 Materials and methods

228 3.1 Chemicals used

229 All chemicals used were of analytical grade or better unless otherwise stated. Methanol (HPLC
230 grade), absolute ethanol, toluene, HCl, NaCl, NaOH, NH₄OH and 3-Aminopropyltriethoxysilane
231 (APTES) were purchased from Fisher Scientific UK Ltd. and ultra-pure (< 1 µS/cm) water was
232 produced from a Millipore ELIX 5 unit (Millipore UK Ltd., UK).

233

234 3.2 Membrane preparation

235 The membrane used was a hydrophobic PTFE microfiltration membrane typically used for filtration
236 and sterilization in medical applications. The membrane has a pore size in the range 45-60 µm and a
237 thickness of 2 mm (Porex Ltd, Aachen, Germany). APTES was coated onto the PTFE membrane via
238 hydrolysis and condensation, using HCl and NH₄OH as catalysts as previously described elsewhere
239 [29]. HCl (0.01 wt%) was added to a mixture of APTES, Ethanol and ultra-pure water (6:89:5), and
240 stirred at 25 °C to ensure dissolution. Following this, 2 wt% NH₄OH was added into the mixture for
241 condensation. The mixture was poured onto the membrane which is held in a mould. The reaction
242 was left to occur at 25 °C for 12 hours. The PTFE membrane was then washed in distilled water and
243 dried for a minimum of 8 hours.

244

245 3.3 Streaming Potential

246 Tangential streaming potential measurements were conducted using an Electrokinetic analyser (EKA)
247 (Anton Paar GmbH, Graz, Austria) using cut flat sheet membranes (2 sheets, 12.5x5.5cm). The
248 electrolyte for this study was aqueous NaCl at concentration of 1 mM. The electrolyte was prepared
249 using ultra-pure water and pH adjusted periodically using 0.1 M HCl and 0.1 M NaOH as required.
250 For methanol – water systems, 1 mM NaCl was dissolved in the mixture and stirred until the NaCl is
251 completely dissolved in the solution. In all cases, fresh electrolyte solution was used for each
252 experiment; even when changing from acidic to alkaline conditions. In this way the concentration of
253 ions in the system is maintained consistent as much as possible. Before loading solutions to the
254 equipment, the system was washed thoroughly with ultra-pure water. Similarly, on entering fresh
255 electrolyte solution to the equipment, a thorough rinse through was conducted to equilibrate the
256 membrane sample. A pressure gradient from 0-700 mbar over 30-seconds was used to produce a
257 streaming current which was recorded using a pair of AgCl electrodes. 10 measurements were made
258 at each pH value using alternating flow directions. Electrolyte pH and conductivity were measured
259 using a pH and conductivity probe. For aqueous solutions, a Fisherbrand pH electrode was used, for
260 alcohol-water solutions a Jenway non-aqueous pH electrode was used. All experiments were
261 conducted at room temperature (25 °C ± 1 °C).

262

263

264 3.4 Laser Doppler Electrophoresis measurements

265 Electrophoretic mobility and electro-osmotic experiments were conducted using a Zetasizer Nano ZS
266 with the surface zeta potential accessory (Malvern, UK) using the methodology described previously
267 [1]. Electrolyte solutions were prepared as described previously but with the addition of 1 drop of
268 0.5 µm negatively charged carboxylated polystyrene latex particles (Polysciences Inc., PA, USA) or
269 0.5 µm positively charged amidine particles (Fisher Scientific Ltd., UK) per 200 mL of electrolyte
270 solution. Membranes were prepared by cutting to shape (3.5 x 5 mm) in order to fit the surface cell
271 and were attached using epoxy (Araldite) resin. Membranes were washed with 5mL of the
272 electrolyte solution to remove any particulate debris before then being submerged into the cuvette.
273 The surface cell was sonicated for 30 seconds in toluene prior to subsequent measurements to
274 remove any debris. This was repeated as necessary until the toluene remained clear. The membrane
275 was then washed with ethanol followed by water and was then dried using compressed air.

276 The Zetasizer conditions use were: forward scatter with the attenuator in position 10, count rate set
277 to the optimal 250-500 kcps range, four distance position measurements in 125 μm steps, three
278 measurements at each location (each measurement consisted of 15 sub-runs with 60s interval),
279 repeat measurements for each pH, and a further three measurements consisting of 100 sub-runs
280 with a 60s interval to measure the electro-osmotic mobility of the tracer particles. All measurements
281 were conducted at 25 $^{\circ}\text{C}$.

282

283 4.0 Results and discussion

284 4.1 Characterisation of the tracer particles

285 The two tracer particles used in this study, latex and amidine, were characterised for surface zeta
286 potential using the Zetasizer Nano ZS and the results are shown in Table 1. As expected, the latex
287 particles demonstrate a strongly negative zeta potential at -52.8 mV. This is in contrast to the
288 Amidine particles that demonstrate a positive zeta potential of 12.4 mV. However, the amidine
289 particles are clearly not as highly charged as the carboxylated latex with only 23% of the charge
290 magnitude. Thus, both particles are confirmed to exhibit the required state of charge for the
291 experimentation.

292

293 4.2 Zeta potential measurements of the PTFE membrane

294 The zeta potential of the raw PTFE membrane was evaluated using both tangential streaming
295 potential and laser Doppler electrophoresis, the results are shown in Figure 3. The zeta potential, as
296 measured from tangential streaming potential, illustrates that the PTFE membrane is positively
297 charged in the low pH range and then rapidly becomes negative as pH is increased, with an
298 isoelectric point in the region of pH 5. At higher pH values, greater than pH 7.5, the zeta potential of
299 the membrane stabilises at about -20 mV. These findings are very similar in trend to those of Wang
300 et al. [29] obtained using KCl as an electrolyte rather than NaCl as in this study. The laser Doppler
301 electrophoresis results when using the negative latex particles show very similar behaviour and are
302 almost identical in trend and magnitude to the tangential streaming potential measurement results.
303 This confirms that the technique is indeed capable of zeta potential measurements of negatively
304 charged membranes as proposed by Thomas et al. [1]. The phase plot and mobility-displacement
305 plot for the measurements are shown in Figure 4. The three average phase measurements are
306 illustrated in Figure 4a and are banded and clear at each of the four displacement lengths used,
307 highlighted by black circles overlaid on the plot. The mobility-displacement is shown in Figure 4b and
308 the surface equivalent mobility was calculated as $-1.411 \mu\text{mcm/Vs}$ ($-[-2.664]+[-4.075]$) with $R^2 =$
309 0.994 . However, care has to be taken when selecting an appropriate tracer particle for use in this
310 measurement technique. In this case, the membrane is negative at the study conditions and so the
311 tracer particle should also be negative. To highlight this problem, the positive Amidine particle was
312 also used to measure the zeta potential of the membrane. The equipment did take a measurement
313 and did derive a zeta potential as a correlation was able to be made. The results are shown in Figure
314 3 as green squares. Clearly the derived zeta potential measurement is very different to that of the
315 other two measurements and is never really anywhere close to the same magnitude or trend. This is
316 problematic when using a membrane of unknown charge. The phase plot and mobility-displacement
317 plot for these measurements are shown in Figure 5a and 5b respectively. In this case the phase plot
318 is not as well defined with each of the lines being quite sporadic and showing no clear trend by
319 comparison with Figure 4a. The surface equivalent mobility for this data set is $-2.36 \mu\text{mcm/Vs}$ ($-$
320 $[0.235]+[-2.125]$) with $R^2 = 0.984$. In this case, the positively charged Amidine particles are adsorbing
321 to the surface of the negatively charged membrane and their mobility in solution is clearly
322 compromised as a result. However, the quality of the mobility-displacement plot (Figure 5b) could
323 easily be interpreted as a good result with the R^2 value being reasonably close to unity. Thus, this

324 data would suggest that avoiding a meaningless result can only be achieved by interpretation of the
325 phase plot when the nature of the surface charge of the membrane is unknown. This would be no
326 issue to an experienced colloid scientist, however, for a less experienced scientist or engineer
327 corroboration of the results obtained from laser Doppler electrophoresis should be made by an
328 alternative technique such as tangential streaming potential and once the nature of the surface is
329 known, laser Doppler electrophoresis can be used with a much higher level of confidence.

330

331 4.3 Zeta potential measurements of the APTES-modified PTFE membrane

332 The PTFE membrane surface charge was adjusted to a positive charge by modification using APTES
333 and the resulting zeta potential derived from tangential streaming potential measurements and laser
334 Doppler electrophoresis are shown in Figure 6. The zeta potential, as measured from tangential
335 streaming potential, illustrates that the APTES-modified PTFE membrane is positively charged at low
336 pH, slowly reduces in charge magnitude as the pH increases and becomes negative beyond a pH of
337 around pH 9. The trend of the zeta potential versus pH is almost linear in fashion. Again, this is very
338 similar behaviour to that observed for a comparable membrane produced by Wang et al. [29]. The
339 zeta potential measurements obtained using laser Doppler electrophoresis and the Amidine particles
340 (positively charged) show very similar behaviour. However, in this case the zeta potential values
341 obtained fall slightly below the values obtained from streaming potential measurements. In essence,
342 the trend is the same but the data is slightly offset and the resulting isoelectric point has moved to
343 around pH 7.8. The phase plot and mobility-displacement were of good quality for the data set (not
344 shown as similar to Figure 4), with the surface equivalent mobility being $0.632 \mu\text{mcm/Vs}$ ($-[-1.494]+[-$
345 $0.862]$) with $R^2 = 0.977$. Interestingly, the magnitude of the charge for the Amidine particle is
346 significantly less than that of the latex particles, see Table 1. This could indicate that better
347 agreement between the laser Doppler electrophoresis and tangential streaming potential
348 measurements could be obtained if a more highly charged positive particle is used and suggests a
349 future study could investigate the quality of the experimental measurement using a variety of
350 particles that span a range in charge magnitude. Overall, both sets of zeta potential data are in
351 reasonable agreement and are certainly suitable for characterisation purposes. The membrane was
352 also characterised using laser Doppler electrophoresis and the negatively charged latex particles, see
353 Figure 6. In this case, the zeta potential for the membrane is now clearly negative, with the
354 magnitude of zeta potential being -30 mV at pH 3.5, decreasing to -75 mV at pH 5.8 and stabilising at
355 this level as pH is increased. This behaviour is in stark contrast to that obtained from the Amidine
356 particles and tangential streaming potential measurements and clearly indicates that the latex
357 particles are adsorbing to the surface of the membrane and modifying the surface charge from
358 positive to negative. The fact that the latex particles are more highly charged than the Amidine
359 particles provides an explanation for this stark deviation, which was not so pronounced for the raw
360 PTFE membrane. The phase plot and mobility-displacement plot for this data are shown in Figure 7a
361 and 7b respectively. As with the counter charged particle data with the unmodified PTFE membrane,
362 the mobility-displacement plot appears to be reasonable with a surface equivalent mobility being $-$
363 $7.086 \mu\text{mcm/Vs}$ ($-[2.11]+[-4.976]$) with $R^2 = 0.982$. Again, when the tracer particle selected carries
364 like charge to the membrane surface, the phase plot is very distorted. However, in this particular
365 case, the very final set of measurements appear quite normal, see Figure 7a circled section. An
366 explanation for this anomaly would be that the counter charge of the latex particle causes
367 adsorption to take place and this adsorption process is fast due to the high magnitude of charge on
368 the latex particle. If this adsorption process was indeed fast enough to conclude prior to the Zeta
369 Sizer machine taking the last set of results, then there would in fact be a negatively charged
370 membrane and residual negatively charged particles in solution. Hence, this would indeed constitute
371 a normal or regular experimental run and the resulting data should indeed be of good quality.

372

373 5.0 Conclusions

374 The novel zeta potential measurement technique using laser Doppler electrophoresis was employed
375 to measure the surface zeta potential of a negatively charge PTFE membrane using latex particles
376 (also negatively charged). The results showed good correlation agreement between mobility-
377 displacement measurements ($R^2 = 0.994$) and a comparison to zeta potential obtained from
378 tangential streaming potential measurements was also in good agreement. Amidine particles were
379 shown to have a positive zeta potential of 12.4 mV and were also used to characterize the PTFE
380 membrane. In this case, the correlation agreement between mobility-displacement measurements
381 was also good ($R^2 = 0.984$), however, the phase diagram indicated significant issues. The resultant
382 zeta potential measurements obtained were in effect meaningless as the positive particles were
383 adsorbing to the negative membrane surface. Thus, when using this new methodology with a
384 surface of unknown charge, care must be taken to ensure the correct tracer particle is used and
385 review of both the mobility-displacement and phase diagram should be made. In the ideal case, a
386 second method for characterization such as tangential streaming potential should also be employed
387 to provide assurance.

388 The PTFE membrane was then modified using APTES to generate a positive surface and this was
389 confirmed across the pH range pH 4 to 9 via tangential streaming potential measurements. The
390 amidine particles were identified as a successful positive tracer particle for use in the laser Doppler
391 electrophoresis experiments allowing zeta potential measurements to be made. A comparative
392 analysis was made between the laser Doppler electrophoresis measurements and tangential
393 streaming potential measurements and the agreement was good, although there was a small
394 amount of offset between the two data sets. The same membrane was then characterized using the
395 latex particles and the data obtained demonstrated that the membrane was once again negatively
396 charged, due to the latex particles strongly adsorbing to the initial positively charged membrane
397 surface.

398 Overall, the work in this paper confirms that laser Doppler electrophoresis is a suitable method for
399 the characterization of membrane surface charge via determination of the membrane surface zeta
400 potential. This technique has several advantages over traditional methodologies that can be
401 beneficial to the development scientist and industrial practitioner alike. This study now expands the
402 methodology to cover positively charged surfaces, which allows the novel technique to span the
403 entire measurement range required for membrane surface charge characterisation.

404

405

406 Acknowledgements

407 This work is part-funded by the European Social Fund (ESF) through the European Union's
408 Convergence programme administered by the Welsh Assembly Government.



409

410



Ysgoloriaethau Sgiliau Economi Gwybodaeth
Knowledge Economy Skills Scholarships

411
412
413
414

References

- 415 [1] T.E. Thomas, S. Al Aani, D.L. Oatley-Radcliffe, P.M. Williams and N. Hilal, Laser Doppler
416 Electrophoresis and electro-osmotic flow mapping: A novel methodology for the
417 determination of membrane surface zeta potential, *Journal of Membrane Science*, 523 (2017)
418 524-532.
- 419 [2] B. Das, B. Chakrabarty and P. Barkakati, Preparation and characterization of novel ceramic
420 membranes for micro-filtration applications, *Ceramics International*, 42(13) (2016) 14326-
421 14333.
- 422 [3] M.I. Khan, A.N. Mondal, B. Tong, C. Jiang, K. Emmanuel, Z. Yang, L. Wu and T. Xu,
423 Development of BPPO-based anion exchange membranes for electro dialysis desalination
424 applications, *Desalination*, 391 (2016) 61-68.
- 425 [4] S. Xu and Y. Wang, Novel thermally cross-linked polyimide membranes for ethanol
426 dehydration via pervaporation, *Journal of Membrane Science*, 496 (2015) 142-155.
- 427 [5] D.L. Oatley-Radcliffe, M. Walters, T.J. Ainscough, P.M. Williams, A.W. Mohammad and N.
428 Hilal, Nanofiltration membranes and processes: A review of research trends over the past
429 decade. *Journal of Water Process Engineering*, 19 (2017) 164-171.
- 430 [6] S. Déon, P. Fievet and C.O. Doubad, Tangential streaming potential/current measurements for
431 the characterization of composite membranes, *Journal of Membrane Science*, 423-424 (2012)
432 413-421.
- 433 [7] S.O. Ganiyu, E.D. Van Hullebusch, M. Cretin, G. Esposito and M.A. Oturan, Coupling of
434 membrane filtration and advanced oxidation processes for removal of pharmaceutical
435 residues: a critical review, *Separation and Purification Technology*, 156 (2015) 891-914.
- 436 [8] G.L. Jadav, V.K. Aswal and P.S. Singh, In-situ preparation of polydimethylsiloxane membrane
437 with long hydrophobic alkyl chain for application in separation of dissolved volatile organics
438 from wastewater, *Journal of membrane Science*, 492 (2015) 95-106.
- 439 [9] F. Zheng, C. Li, Q. Yuan and F. Vriesekoop, Influence of molecular shape on the retention of
440 small molecules by solvent resistant nanofiltration (SRNF) membranes: A suitable molecular
441 size parameter, *Journal of Membrane Science*, 318(1-2) (2008) 114-122.
- 442 [10] F. Zheng, Z. Zhang, C. Li and Q. Yuan, A comparative study of suitability on different molecular
443 size descriptors with the consideration of molecular geometry in nanofiltration, *Journal of*
444 *Membrane Science*, 332(1-2) (2009) 13-23.
- 445 [11] D.L. Oatley, L. Llenas, N.H. Aljohani, P.M. Williams, X. Martinez-Lladó, M. Rovira and J. de
446 Pablo, Investigation of the dielectric properties of nanofiltration membranes, *Desalination*,
447 315 (2013) 100-106.
- 448 [12] D.L. Oatley-Radcliffe, S.R. Williams, T.J. Ainscough, C. Lee, D.J. Johnson and P.M. Williams,
449 Experimental determination of the hydrodynamic forces within nanofiltration membranes and
450 evaluation of the current theoretical descriptions, *Separation and Purification Technology*, 149
451 (2015) 339-348.

- 452 [13] N. Hilal, A.F. Ismail, T. Matsuura and D.L. Oatley-Radcliffe, eds., 2017. Membrane
453 Characterization. Elsevier.
- 454 [14] R. Xu, Shear plane and hydrodynamic diameter of microspheres in suspension, *Langmuir*, 14
455 (1998) 2593-2597.
- 456 [15] B.D. Coday, T. Luxbacher, A.E. Childress, N. Almaraz, P. Xu and T.Y. Cath, Indirect
457 determination of zeta potential at high ionic strength: Specific application to semipermeable
458 polymeric membranes, *Journal of Membrane Science*, 478 (2015) 58-64.
- 459 [16] A. Al-Amoudi and R.W. Lovitt, Fouling strategies and the cleaning system of NF membranes
460 and factors affecting cleaning efficiency, *Journal of Membrane Science*, 303(1-2) (2007) 4-28.
- 461 [17] A. Almojjly, D. Johnson, D.L. Oatley-Radcliffe and N. Hilal, Removal of oil from oil-water
462 emulsion by hybrid coagulation/sand filter as pre-treatment, *Journal of water process
463 engineering*, 26 (2018) 17-27.
- 464 [18] S. Cheng, D.L. Oatley, P.M. Williams and C.J. Wright, Characterisation and application of a
465 novel positively charged nanofiltration membrane for the treatment of textile industry
466 wastewaters, *Water research*, 46(1) (2012) 33-42.
- 467 [19] D.J. Johnson, D.L. Oatley-Radcliffe and N. Hilal, State of the art review on membrane surface
468 characterisation: Visualisation, verification and quantification of membrane properties,
469 *Desalination*, 434 (2018) 12-36.
- 470 [20] D.L. Oatley-Radcliffe, N. Aljohani, P.M. Williams and N. Hilal, 2017. Electrokinetic Phenomena
471 for Membrane Charge. In *Membrane Characterization* (pp. 405-422). Elsevier.
- 472 [21] J.C. Corbett, F. McNeil-Watson, R.O. Jack and M. Howarth, Measuring surface zeta potential
473 using phase analysis light scattering in a simple dip cell arrangement, *Colloids and Surfaces A;
474 Physicochemical and Engineering Aspects*, 396 (2012) 169-176.
- 475 [22] I.M. Tucker, J.C.W. Corbett, J. Fatkin, R.O. Jack, M. Kaszuba, B. MacCreath and F. McNeil-
476 Watson, Laser Doppler Electrophoresis applied to colloids and surfaces, *Current Opinions in
477 Colloid Interface Science*, 20 (2015) 215–226.
- 478 [23] N.J.W. Penfold, A.J. Parnell, M. Molina, P. Verstraete, J. Smets and S.P. Armes, Layer-by-layer
479 self-assembly of polyelectrolytic block copolymer worms on a planar substrate, *Langmuir*, 33
480 (2017) 14425-14436.
- 481 [24] A. Szymczyk, Y.I. Dirir, M. Picot, I. Nicolas and F. Barrière, Advanced electrokinetic
482 characterization of composite porous membranes, *Journal of Membrane Science*, 429 (2013)
483 44–51.
- 484 [25] Y. Hanafi, P. Loulergue, S. Ababou-Girard, C. Meriadec, M. Rabiller-Baudry, K. Baddari and A.
485 Szymczyk, Electrokinetic analysis of PES/PVP membranes aged by sodium hypochlorite
486 solutions at different pH, *Journal of Membrane Science*, 501 (2016) 24–32.
- 487 [26] D.G. Dalgleish, Measurement of electrophoretic mobilities and zeta-potentials of particles
488 from milk using laser Doppler electrophoresis, *Journal of Dairy Research*, 51 (1984) 425–438.
- 489 [27] A.V. Delgado, F. Gonzalez-Caballero, R.J. Hunter, L.K. Koopal and J. Lyklema, Measurement and
490 interpretation of electrokinetic phenomena, *Journal of Colloid Interface Science*, 309 (2007)
491 194–224.
- 492 [28] J.W. Swan and E.M. Furst, A simpler expression for Henry's function describing the
493 electrophoretic mobility of spherical colloids, *Journal of Colloid Interface Science*, 388 (2012)
494 92–94.
- 495 [29] F. Wang, H. Zhu, H. Zhang, H. Tang, J. Chen and Y. Guo, Effect of surface hydrophilic
496 modification on the wettability, surface charge property and separation performance of PTFE
497 membrane, *Journal of water process engineering*, 8 (2015) 11-8.

498 [30] H. Bukšek, T. Luxbacher, and I. Petrinić, Zeta potential determination of polymeric materials
499 using two differently designed measuring cells of an electrokinetic analyzer. *Acta chimica*
500 *slovenica*, 57(3) (2010) 700-706.

501

502 **Figures and Tables**

503 **Figure 1:** A representation of the electrical double layer model describing potential as a
504 function of distance from the membrane surface.

505 **Figure 2:** The Uzgiris dip cell arrangement used in electro-osmotic flow mapping for surface zeta
506 potential measurements.

507 **Figure 3:** Zeta potential measurements for the unmodified PTFE membrane using both tangential
508 streaming potential (TSP) and laser Doppler electrophoresis (Zeta Sizer).

509 **Figure 4:** Information derived from the laser Doppler electrophoretic measurements for the
510 unmodified PTFE membrane using latex particles (negatively charged), a) the phase plot and b)
511 mobility-displacement plot.

512 **Figure 5:** Information derived from the laser Doppler electrophoretic measurements for the
513 unmodified PTFE membrane using Amidine particles (positively charged), a) the phase plot and b)
514 mobility-displacement plot.

515 **Figure 6:** Zeta potential measurements for the APTES modified PTFE membrane using both
516 tangential streaming potential (TSP) and laser Doppler electrophoresis (Zeta Sizer).

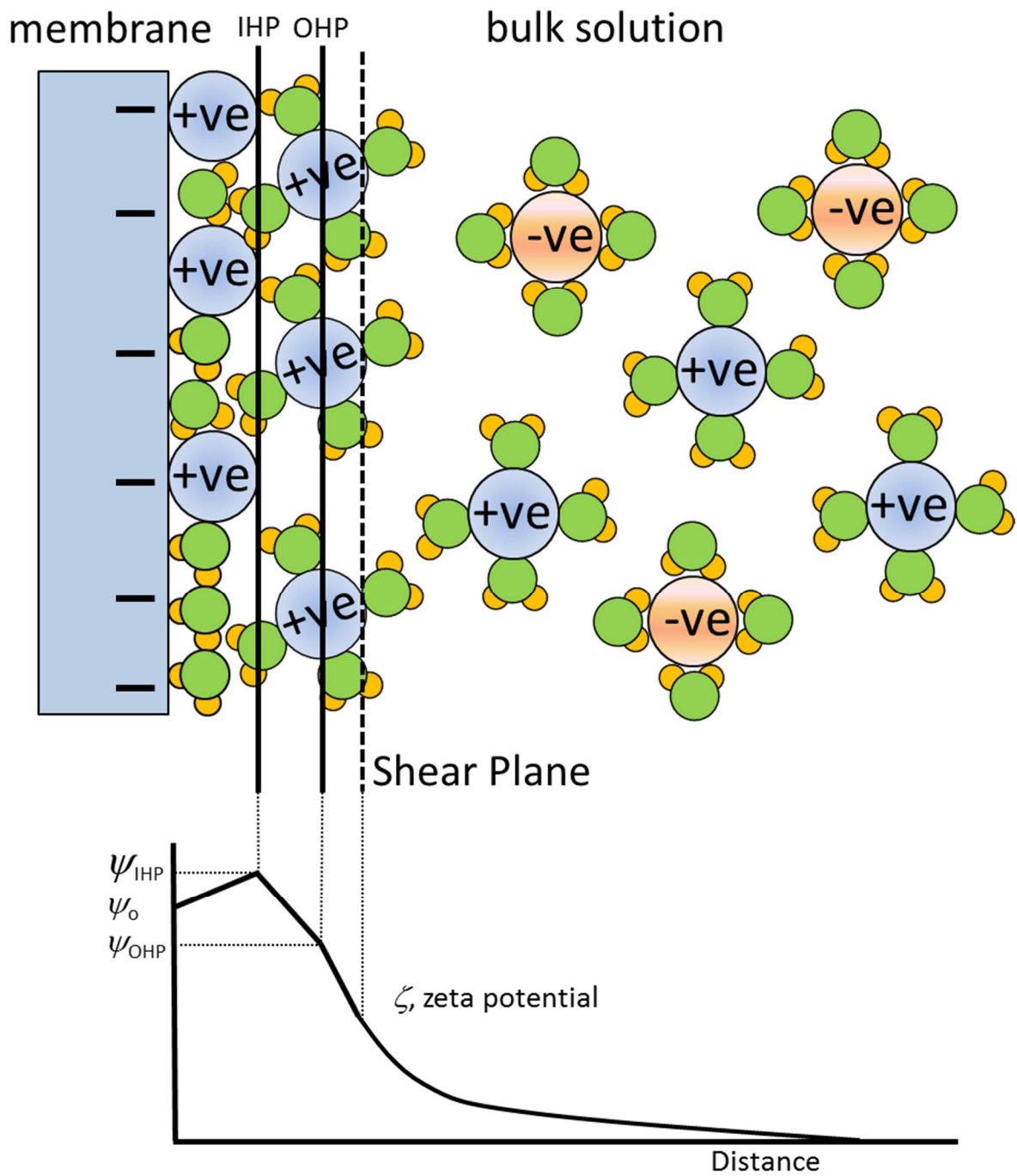
517 **Figure 7:** Information derived from the laser Doppler electrophoretic measurements for the APTES-
518 modified PTFE membrane using latex particles (negatively charged), a) the phase plot and b)
519 mobility-displacement plot.

520

521 **Table 1:** Characterisation data for the tracer particles.

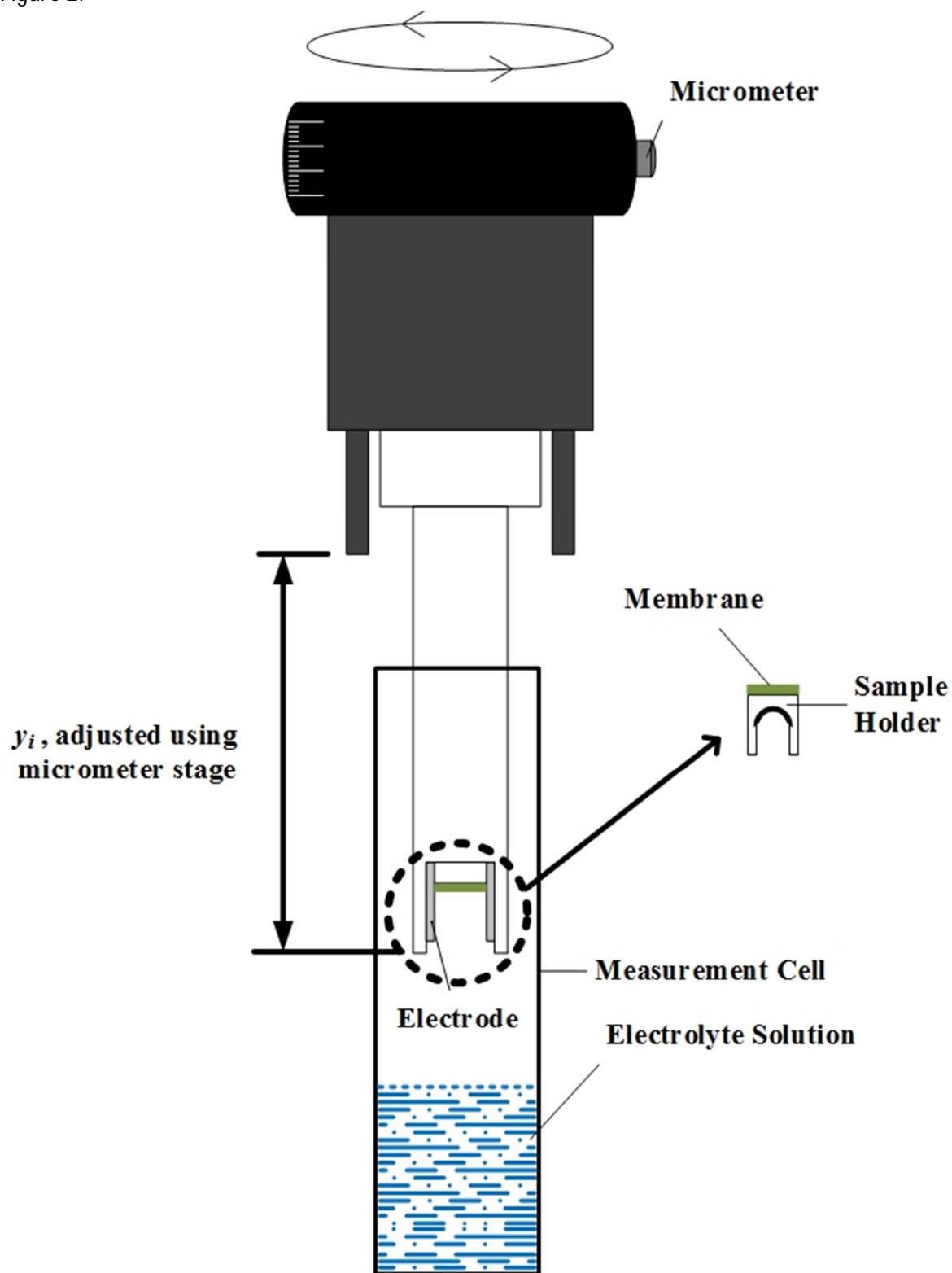
Journal Pre-proof

522 Figure 1:

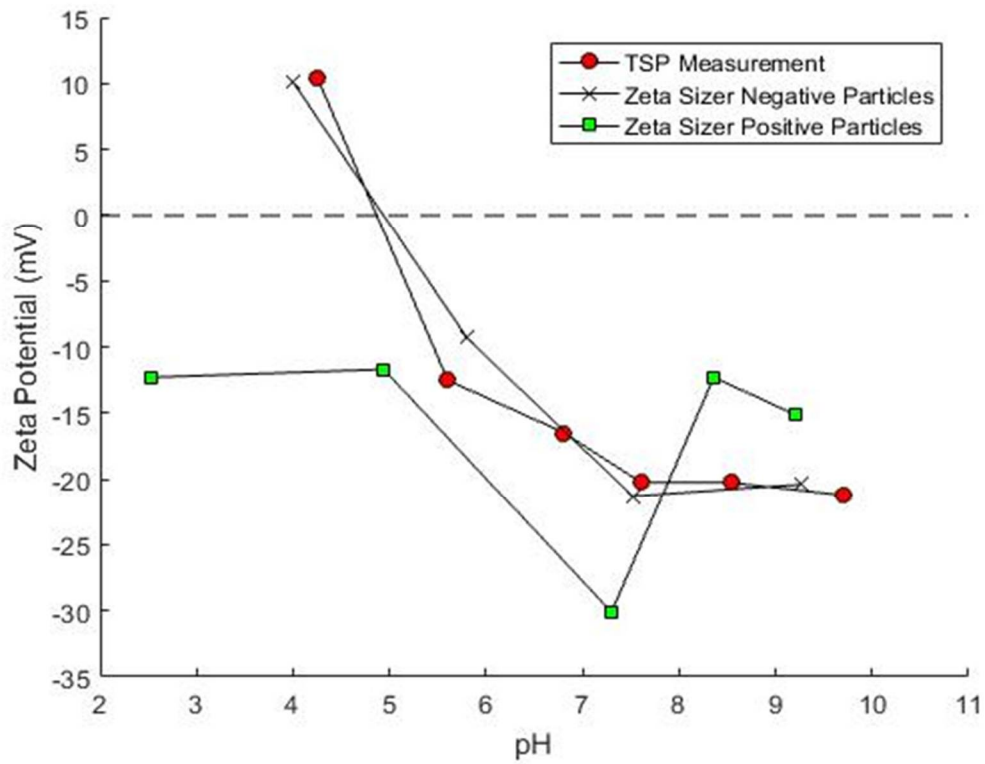


523
 524
 525

526 Figure 2:

527
528
529
530

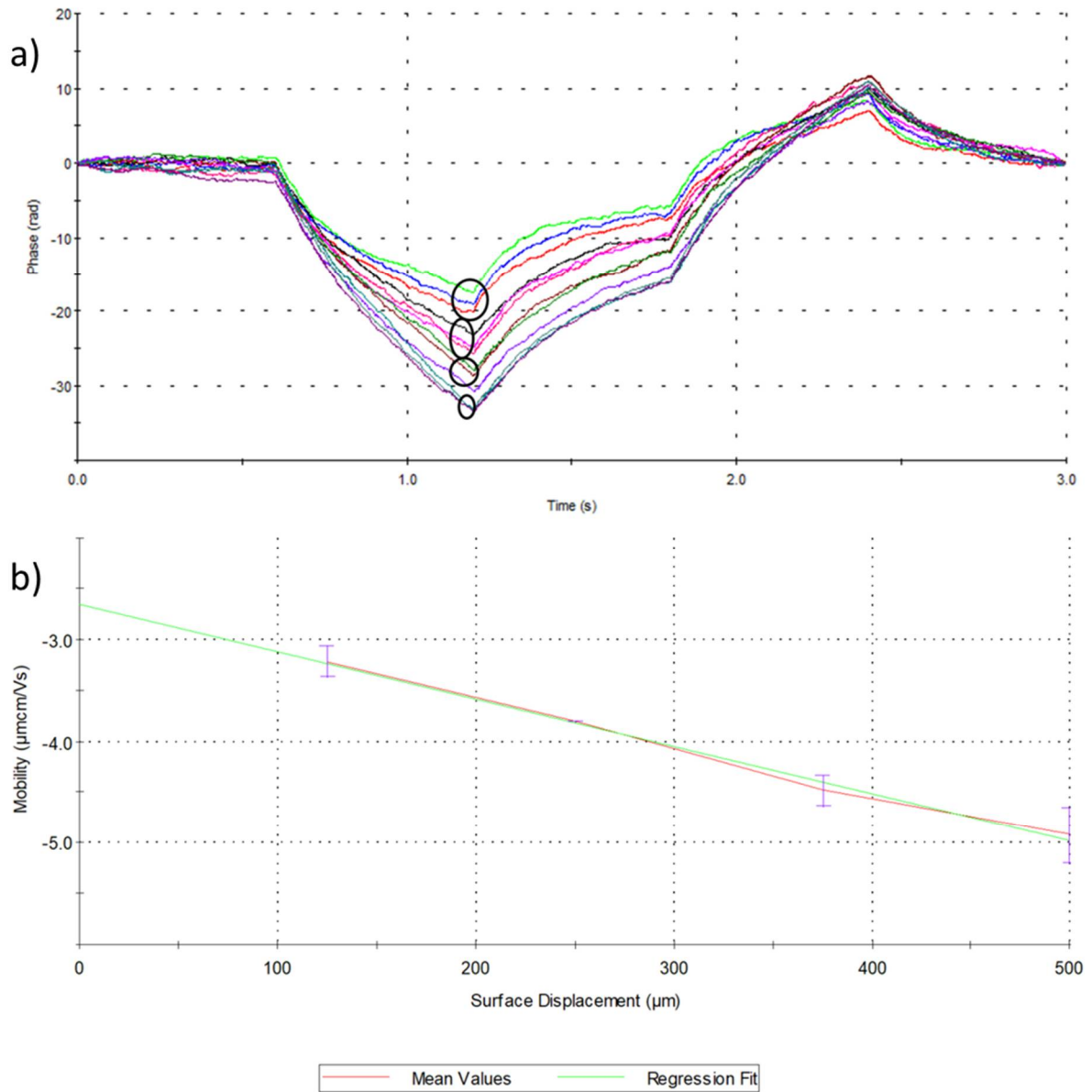
531 Figure 3:
532



533

Journal Pre-proof

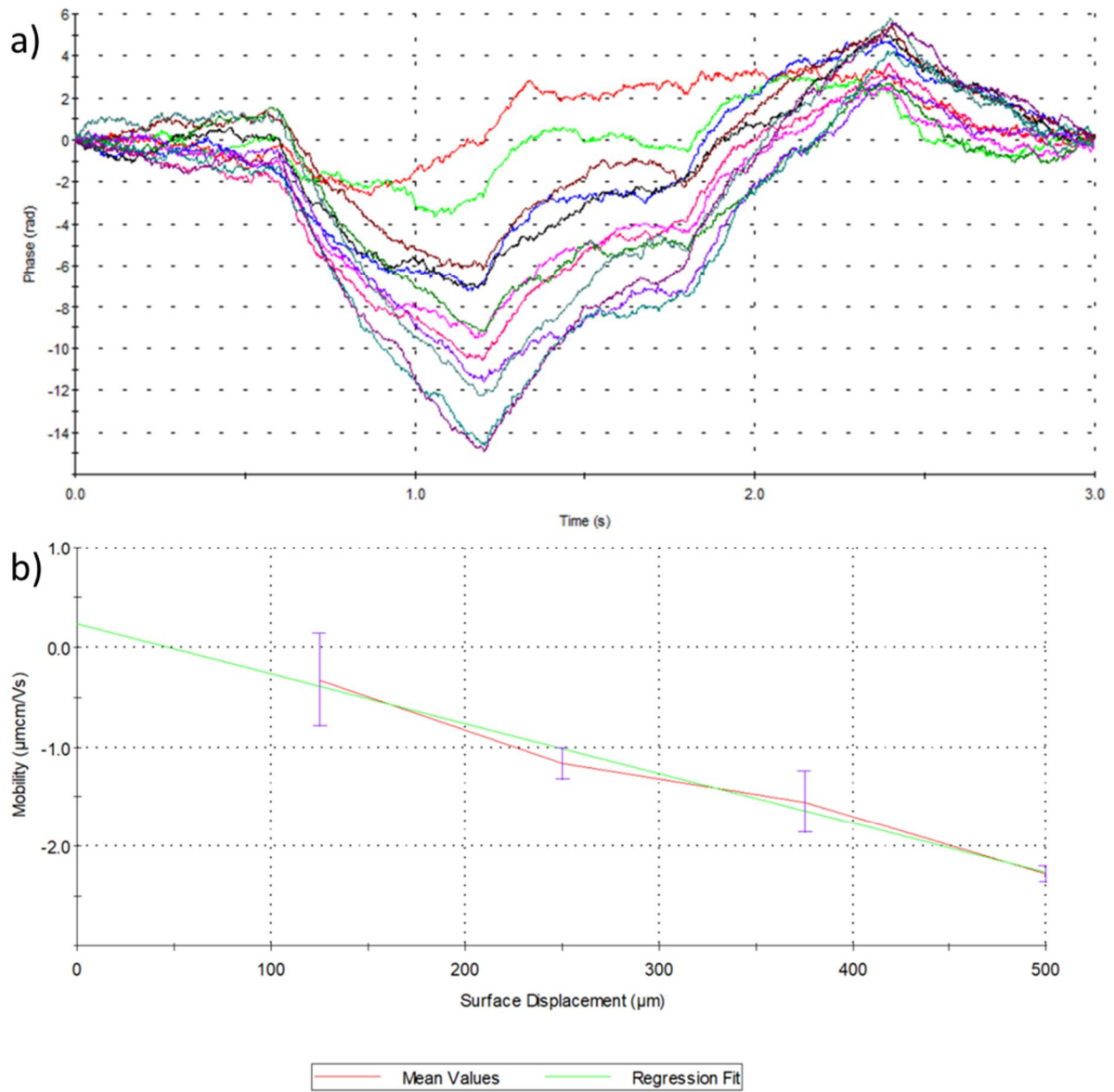
534 Figure 4:
535



536
537
538
539
540
541

Journal

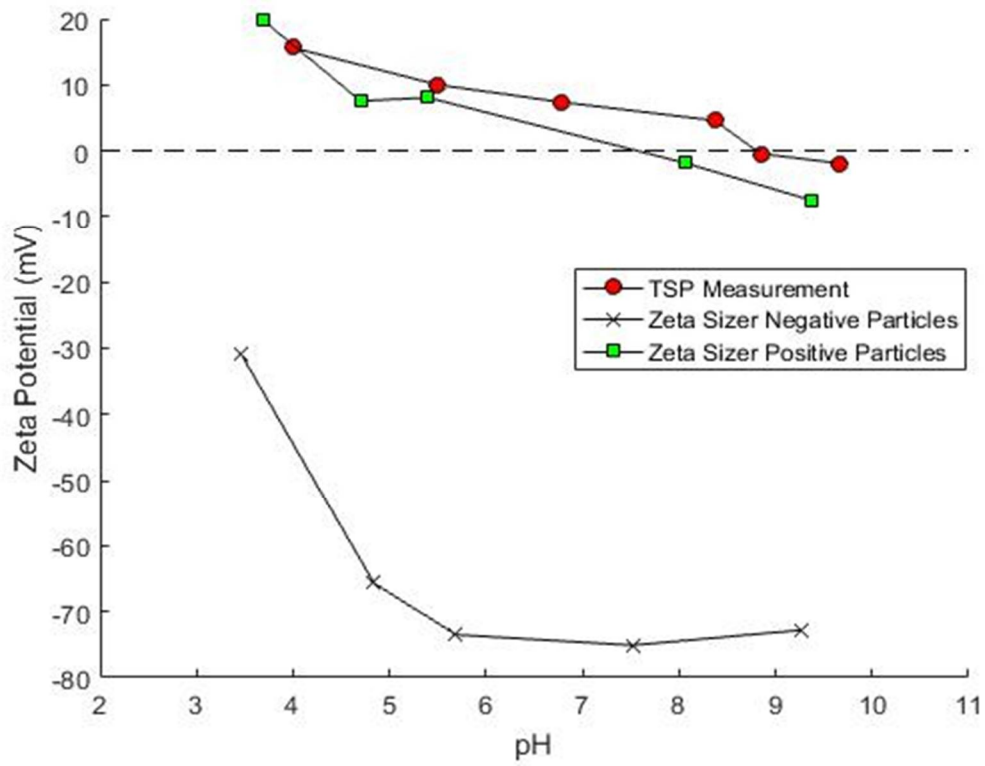
542 Figure 5:
543



544
545
546
547

Journal

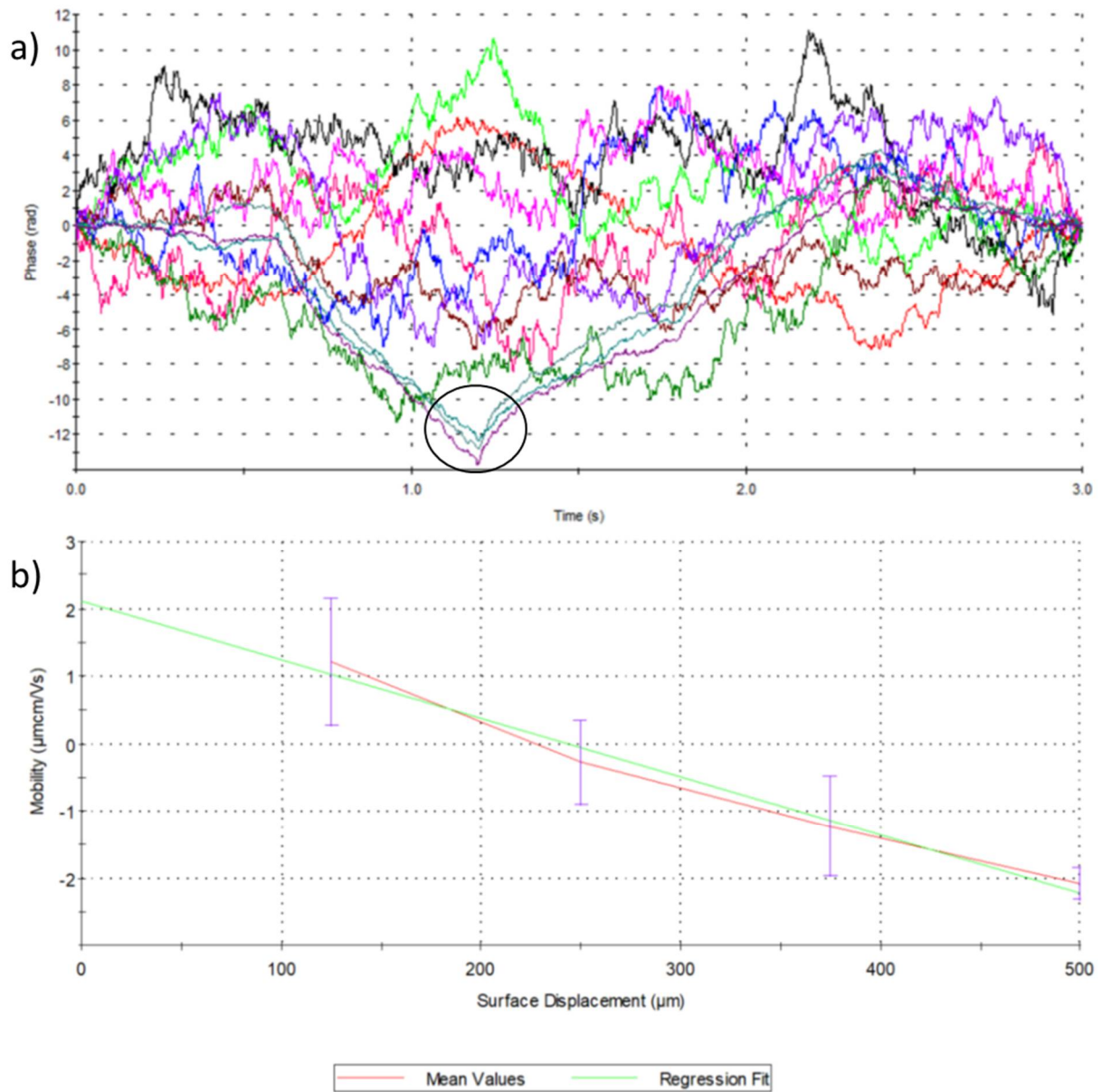
548 Figure 6:



549
550
551
552
553

Journal Pre

554 Figure 7:



555
556
557
558

Journal

559 Table 1:
560

<i>Parameter/Particle</i>	<i>Latex</i>	<i>Amidine</i>
<i>Zeta Potential (mV)</i>	-52.8	12.4
<i>Standard Deviation</i>	8.56	2.83
<i>Mobility ($\mu\text{mcm/Vs}$)</i>	-4.119	0.784
<i>Conductivity (mS/cm)</i>	0.192	0.104

561
562
563
564
565

Highlights

- 566
- Laser Doppler Electrophoresis was successfully applied to positively charged membranes
 - Laser Doppler Electrophoresis was successful for membrane charge characterization
 - Results were compared to Streaming Potentials and found to correlate well
 - The novel technique now spans the entire membrane range
- 567
568
569
570

Journal Pre-proof

Graphical abstract

